

# Wetting behavior of $Zr_{55}Cu_{30}Al_{10}Ni_5$ melt on alumina<sup>①</sup>

XU Qian-gang(徐前刚)<sup>1, 2</sup>, ZHANG Hai-feng(张海峰)<sup>2</sup>, HU Zhuang-qi(胡壮麒)<sup>2</sup>  
(1. Department of Materials Science and Engineering,

Shenyang Institute of Aeronautic Engineering, Shenyang 110034, China;

2. Shenyang National Laboratory for Materials Science, Institute of Metal Research,  
The Chinese Academy of Sciences, Shenyang 110016, China)

**Abstract:** The wetting behavior of molten  $Zr_{55}Cu_{30}Al_{10}Ni_5$  on  $Al_2O_3$  was studied by the sessile drop method in high vacuum. The results show that wetting kinetic at 1 163 K is composed of three stages: incubation, quasi-steady decrease and trend constant. Precursor film forms surrounding the wetting tip when wetting temperature is above 1 163 K. Formation of precursor film is related to the change of triple line configuration and results in good wettability. Chemical reaction does not occur at the wetting interface.  $Al_2O_3$  is an excellent reinforcement for  $Zr_{55}Cu_{30}Al_{10}Ni_5$  matrix composite in terms of wettability and reactivity. The kinetic relationship of spreading ratio with spreading time was also investigated.

**Key words:** wetting; interfacial reaction; precursor film

**CLC number:** TG 113.26; TG 139.8

**Document code:** A

## 1 INTRODUCTION

Wetting of ceramic by molten metals is one of the most important phenomena to be considered when designing a metal matrix composite. Wettability and reactivity determine the quality of the bonding between the constituents and, thereby, greatly affect the final properties of the composite<sup>[1-4]</sup>. Therefore, in order to produce metal-ceramic composites by liquid-phase processing it is necessary to characterize the wetting behavior of molten metals on ceramics.

Investigations of multicomponent deep eutectic metallic systems have led to the development of bulk metallic glasses with extremely high glass forming ability. Some studies have indicated that bulk metallic glass formers are excellent matrix materials for composites<sup>[5-7]</sup>. Some bulk metallic glass matrix composites had been synthesized by melt infiltration casting. A good reinforcement should have good wettability and controllable reactivity with bulk metallic glass formers, and have little effect on the glass forming ability of matrix. However, as a new kind of matrix material, data on wettability of these molten alloys on reinforcements are rather scarce. Alumina particles or fibers are usually used as reinforcement for metal matrix composites.  $Zr_{55}Cu_{30}Al_{10}Ni_5$  alloy is one of the potential bulk metallic glass matrix materials for composites. In this study, wetting behavior of  $Zr_{55}Cu_{30}Al_{10}Ni_5$  melt on alumina was investigated.

The possibility of alumina as reinforcement for  $Zr_{55}Cu_{30}Al_{10}Ni_5$  metallic glass matrix was discussed from the view point of wettability and reactivity.

## 2 EXPERIMENTAL

### 2.1 Materials and method

$Zr_{55}Cu_{30}Al_{10}Ni_5$  (molar fraction, %) alloy was prepared by arc melting a mixture of Zr, Cu, Ni and Al in an argon atmosphere. Of the metals used, Zr and Cu were of > 99.999% purity, and Al and Ni were of > 99.99% purity.

The ceramic substrates used in this work were hot-pressed sintered alumina. The surface of the substrates was polished with SiC powder and 1.5  $\mu$ m diamond paste before used. The chemical compositions of alumina substrate are 99.0%  $Al_2O_3$ , 0.4% MgO and 0.6%  $SiO_2$ .

The sessile drop method was employed to measure the contact angle between the melt and oxide substrate at the temperature range from 1 153 K to 1 273 K. The apparatus consists essentially of a molybdenum resistance furnace fitted with two windows, enabling the illumination of the sessile drop on the substrate and the projection of its image on a screen. The dimensions required for the calculations of the contact angles and spreading ratio were measured directly from the image of the drop section.

All of the wetting experiments were done in

① **Foundation item:** Project(G2000067201) supported by the National Basic Research Program of China

**Received date:** 2004 - 04 - 20; **Accepted date:** 2004 - 11 - 20

**Correspondence:** XU Qian-gang, Associate Professor, PhD; Tel: + 86-24-86142017; E-mail: qgxu@imr.ac.cn

vacuum of  $1.8 \times 10^{-3}$  Pa. The samples were cooled under vacuum by turning off the heater. After completion of the sessile drop experiments, the solidified samples were sectioned and polished to examine the  $\text{Zr}_{55}\text{Cu}_{30}\text{Al}_{10}\text{Ni}_5/\text{Al}_2\text{O}_3$  interfaces by scanning electron microscopy (SEM) and electron probe micro analyzer (EPMA). Some of the samples were etched in the chemical solution (90%  $\text{HNO}_3$  + 10%  $\text{HF}$ ). In order to identify the interfacial reaction product, after the solidified droplet was separated from the oxide substrate mechanically, the surface of the interaction layer on the substrate was analyzed by X-ray diffractometry (XRD).

## 2.2 Definition of spreading ratio

The sessile drop method is an effective method to investigate the wetting and spreading between liquid and solid. Much valuable information can be obtained from it, such as the surface tension of liquid phase, wetting angle of liquid-solid interface, the spreading area and radius. In previous studies on spreading kinetics, the spreading radius was usually measured as an object of study<sup>[8, 9]</sup>. Evidently the difference masses of the drop would result in differences in the spreading radius. The change of spreading area per unit mass with different time was also measured to describe the spreading kinetics. But this treatment is influenced by the drop mass too. For example, supposing the liquid drop is spherical cap, two drops 1 and 2 possess the same density ( $\rho$ ), the volume ratio of the two droplets is  $\phi$ , i. e.  $V_1/V_2 = \phi$ . If the wetting angle ( $\theta$ ) of them with the solid substrates are alike, the two spread areas per unit mass are given by  $S'_1 = \pi R_1^2 \sin^2 \theta / (V_1 \rho)$  and  $S'_2 = \pi R_2^2 \sin^2 \theta / (V_2 \rho)$ , respectively, where  $R_1$  and  $R_2$  are the principal radii of the two spherical caps, respectively. Then  $S'_1/S'_2 = \phi^{-1/3}$ , therefore the volume of the droplet is larger and the spread area per unit mass is smaller.

To make the experimental values of the various volume drops be comparable with each other and have no effect on the law of the spreading kinetics, we take the ratio of the spreading area ( $S$ ) in the experimental process to the intrinsic cover area ( $S_0$ ) of the drop (the equatorial plane of liquid drop when  $\theta = 180^\circ$ ) as the spreading ratio ( $\alpha$ ) of liquid on solid. As mentioned above, the two intrinsic cover areas are given by  $S_{01} = \pi R_{01}^2$  and  $S_{02} = \pi R_{02}^2$ , then  $S_{01}/S_{02} = \phi^{2/3}$ . When two wetting angles are the same, the spreading areas of drops 1 and 2 are given by  $S_1 = \pi R_1^2 \sin^2 \theta$  and  $S_2 = \pi R_2^2 \sin^2 \theta$ , then  $\alpha_1/\alpha_2 = S_1 S_{02} / S_{01} S_2 = \phi^{2/3} \phi^{-2/3} = 1$ , therefore the spreading ratio  $\alpha$  of various mass samples is the same for the same system and experimental condition. In this paper, kinetic relationship of the spreading ratio  $\alpha$  of the  $\text{Zr}_{55}\text{Cu}_{30}\text{Al}_{10}\text{Ni}_5/\text{Al}_2\text{O}_3$  sys-

tem with wetting time was investigated.

## 3 RESULTS AND DISCUSSION

### 3.1 Wettability

Fig. 1 shows a typical example of the contact angle as a function of time for the wetting of  $\text{Al}_2\text{O}_3$  by  $\text{Zr}_{55}\text{Cu}_{30}\text{Al}_{10}\text{Ni}_5$  melt. The relation curve of  $\theta$  against  $t$  at 1 163 K is composed of three stages: incubation, quasi-steady decrease and trend constant. At 1 153 K, the wetting angle is larger than  $90^\circ$  and holds constant. When the wetting temperature is 1 193 K, incubation stage vanishes, and  $\theta$  decreases at a larger slope during the initial stage.

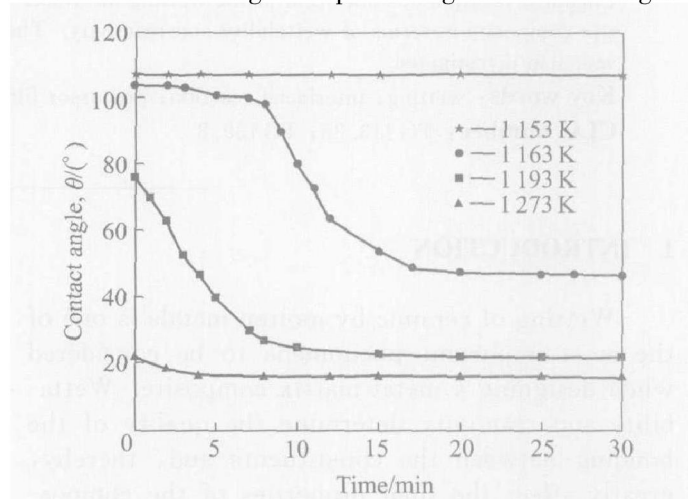
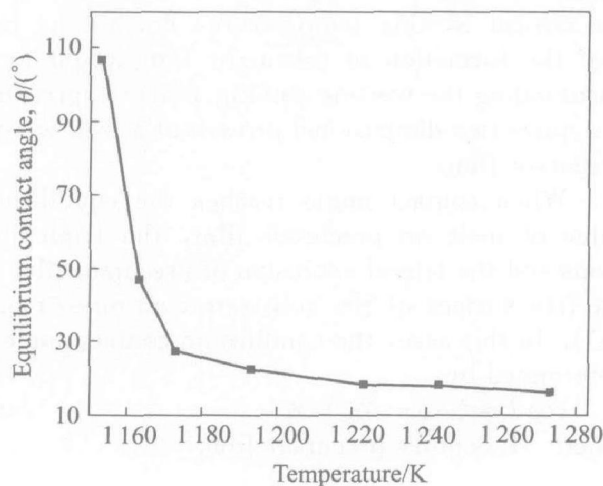


Fig. 1 Variation of contact angle  $\theta$  with time  $t$  for molten  $\text{Zr}_{55}\text{Cu}_{30}\text{Al}_{10}\text{Ni}_5$  on  $\text{Al}_2\text{O}_3$  at various temperatures

The equilibrium contact angle  $\theta_e$  as a function of temperature is shown in Fig. 2. It is clear that the equilibrium contact angle decreases dramatically when the wetting temperature increases from 1 153 K to 1 173 K and then decreases slowly with increasing temperature. The equilibrium contact angle is about  $16^\circ$  at high temperatures, which is much lower than that of typical metal-ceramic system. Small contact angle means that  $\text{Al}_2\text{O}_3$  is an excellent material for using as reinforcement for  $\text{Zr}_{55}\text{Cu}_{30}\text{Al}_{10}\text{Ni}_5$  bulk metallic glass matrix composites from the viewpoint of wettability.

Precursor film forms surrounding the wetting tip of  $\text{Al}_2\text{O}_3$  by  $\text{Zr}_{55}\text{Cu}_{30}\text{Al}_{10}\text{Ni}_5$  melt when the wetting temperature is higher than 1 163 K. Figs. 3(a) and (b) show the top view and cross-sectional view of the precursor film, respectively. EPMA results indicate that the precursor film mainly consists of Zr and Cu. The width of precursor film is sensitive to the experimental condition and has a larger difference even for the same temperature and holding time. It is difficult to analyze the effect of temperature and holding time on the growth of the precursor film. In this study the narrow precursor



**Fig. 2** Equilibrium contact angle of molten  $Zr_{55}Cu_{30}Al_{10}Ni_5$  on  $Al_2O_3$  as function of temperature

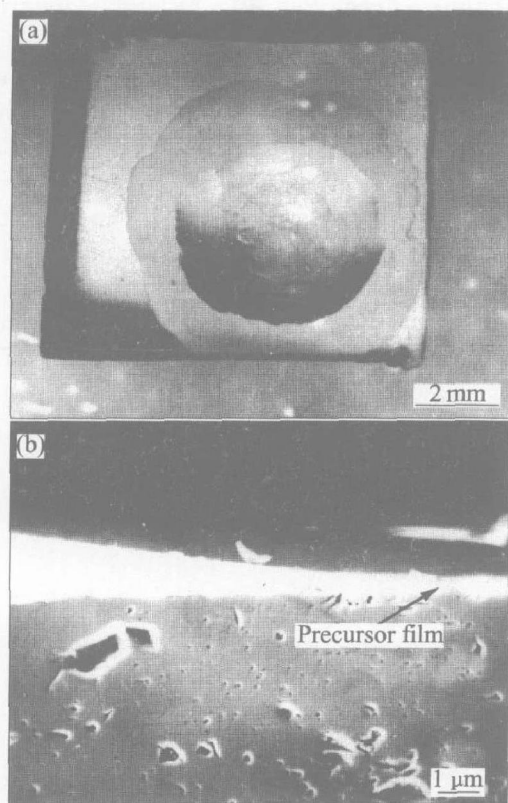


**Fig. 3** Images of precursor film formed in wetting of  $Al_2O_3$  by molten  $Zr_{55}Cu_{30}Al_{10}Ni_5$   
 (a) —Top view of sample at 1223 K for 3 min;  
 (b) —Cross-section view of sample at 1223 K for 30 min

film is about 20  $\mu m$  in width, but the broad one is about 2 mm in width. Precursor film is usually observed in the metal-metal system, such as the wetting of Sn-Pb solder on Cu sheet and 72Ag-28Cu solder on 1Cr18Ni9 stainless steel<sup>[10, 11]</sup>. However, precursor film has only been detected in several special liquid metal-ceramic systems, such as the wetting of  $Cu_{50}Ti_{50}$  solder on Sialon and Sn-base active solder containing Ti or Zr on Sialon<sup>[12, 13]</sup>. It

has been proposed that such films result from the diffusion of melt over the surface of the solid. The formation of precursor film depends on the kinds of melt and substrate.

Fig. 4 shows the SEM images taken from cross-section perpendicular to the interface in  $Zr_{55}Cu_{30}Al_{10}Ni_5/Al_2O_3$  after wetting experiment. No reaction product has been detected at the  $Zr_{55}Cu_{30}Al_{10}Ni_5/Al_2O_3$  interface from the results of XRD analysis at the wetting interface (Fig. 5) and SEM images. However, in some authors' studies about the wetting and interfacial reaction of  $Al_2O_3$  with brazing alloys containing Zr, such as Ag-28% Cu-5% Zr and Ag-Ir-(0.36–10)% Zr, they found the formation of a reaction layer of  $ZrO_2$  because of a redox reaction between Zr in the brazing alloy and  $Al_2O_3$ <sup>[14, 15]</sup>. The effectiveness of Zr as a reactive metal is linked to its higher activity coefficient in those brazing alloys. However, there is a higher affinity for Zr to other elements in  $Zr_{55}Cu_{30}Al_{10}Ni_5$  melt. The microstructural observation and EPMA results indicate that a larger volume fraction of intermetallic compound ( $Zr_2Cu$ ,  $Zr_2Ni$ ) is evident in the main body of  $Zr_{55}Cu_{30}Al_{10}Ni_5$  alloy. Higher affinity to other elements would decrease evidently the activity of Zr in  $Zr_{55}Cu_{30}Al_{10}Ni_5$  melt. Hence, it is not feasible to form  $ZrO_2$  at the interface between  $Zr_{55}Cu_{30}Al_{10}Ni_5$  melt and  $Al_2O_3$ .  $Al_2O_3$  is also an excellent reinforcement for  $Zr_{55}Cu_{30}Al_{10}Ni_5$  bulk metallic glass matrix composite in terms of interfacial reactivity.

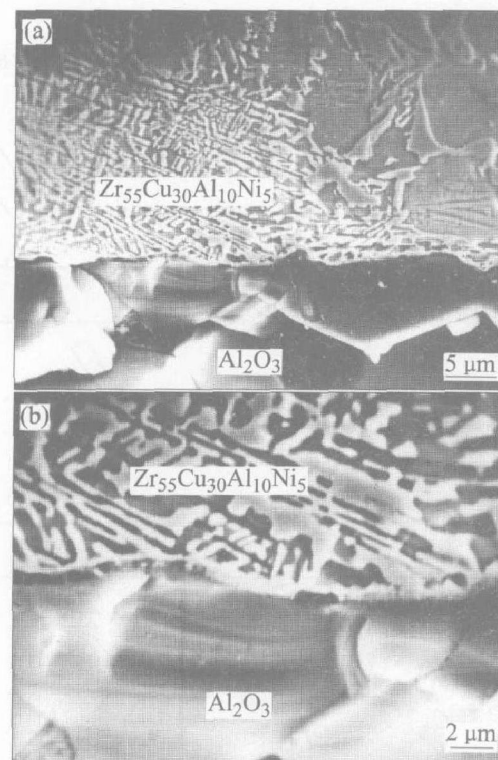


**Fig. 4** Interfacial morphology in  $Zr_{55}Cu_{30}Al_{10}Ni_5/Al_2O_3$  wetting system at 1223 K for 10 min

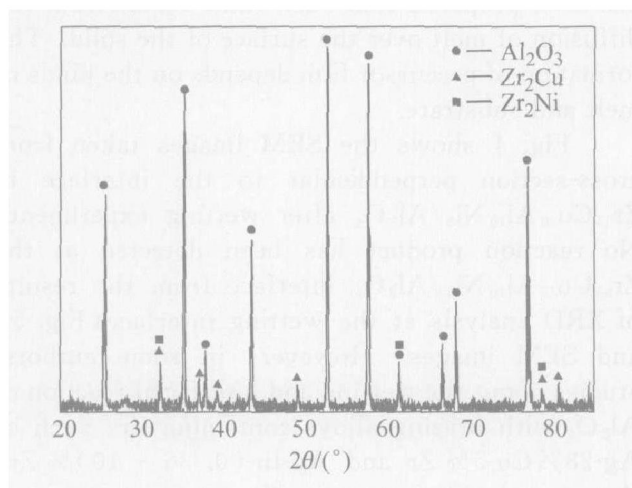


**Fig. 5** X-ray diffraction pattern (Cu K $\alpha$  radiation) of Zr<sub>55</sub>Cu<sub>30</sub>Al<sub>10</sub>Ni<sub>5</sub>/Al<sub>2</sub>O<sub>3</sub> wetting interface at 1 223 K for 30 min

Formation of precursor film usually results in a good wettability. Good wettability of Zr<sub>55</sub>Cu<sub>30</sub>Al<sub>10</sub>Ni<sub>5</sub> melt on Al<sub>2</sub>O<sub>3</sub> is also related to the formation of precursor film. In order to explain this characteristic phenomenon, a schematic diagram is drawn in Fig. 6. The driving force for wetting correlates with the triple line configuration<sup>[16]</sup>. Although no new phase forms at the liquid/solid interface, the formation of precursor film can change the interfacial chemistry at the triple line. Below the critical wetting temperature, precursor film can not form (Fig. 6(b) and Fig. 6(c)) and the equilibrium contact angle is given by the following equation:

$$\cos \theta_e = (\gamma_{SV} - \gamma_{SL}) / \gamma_{LV} \quad (1)$$

where  $\gamma$  is the interfacial tension, S denotes the

Al<sub>2</sub>O<sub>3</sub> substrate, L liquid and V vapour. Above the critical wetting temperature, due to the fact that the formation of precursor film would form surrounding the wetting tip (Fig. 6(d)), spreading is a quasi two-dimensional growth of a well wetted precursor film.

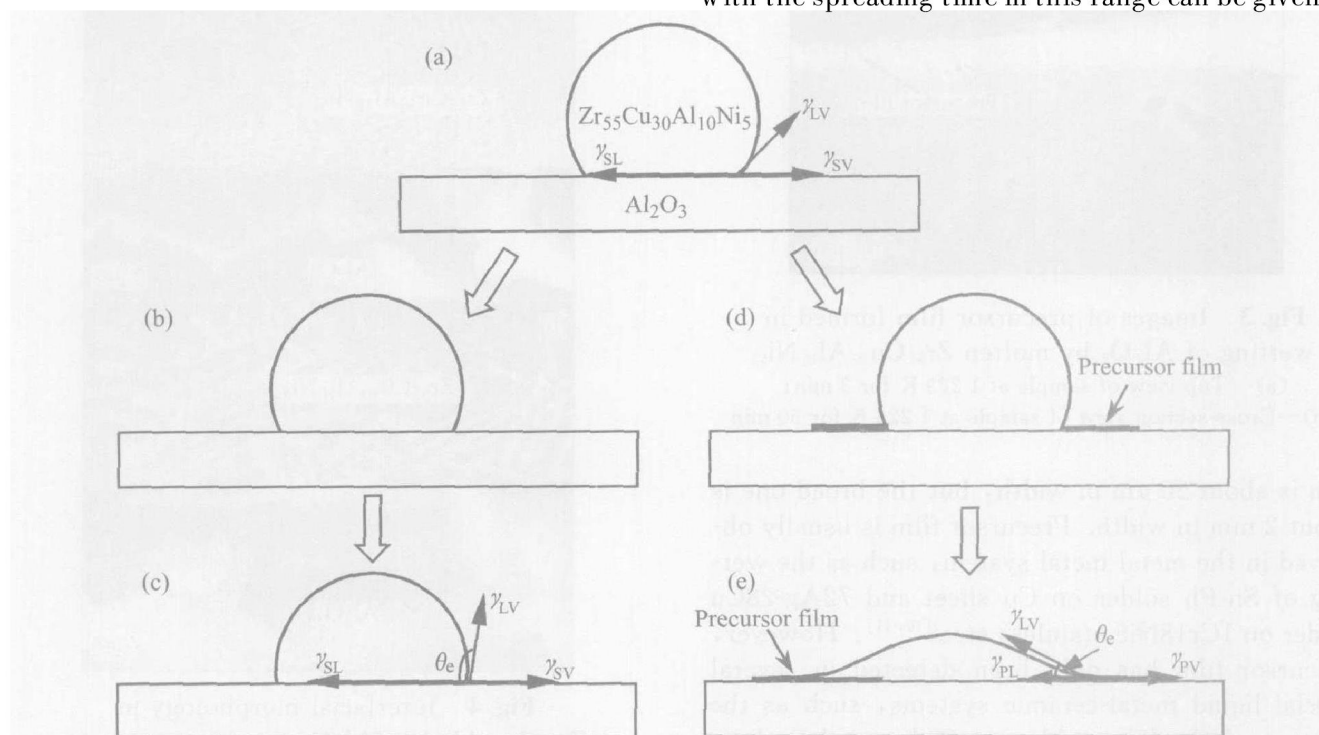
When contact angle reaches the equilibrium value of melt on precursor film, the triple line stops and the lateral extension of precursor film on the free surface of the substrate continues (Fig. 6(e)). In this case, the equilibrium contact angle is determined by:

$$\cos \theta_e = (\gamma_{PV} - \gamma_{PL}) / \gamma_{LV} \quad (2)$$

where P denotes precursor film.

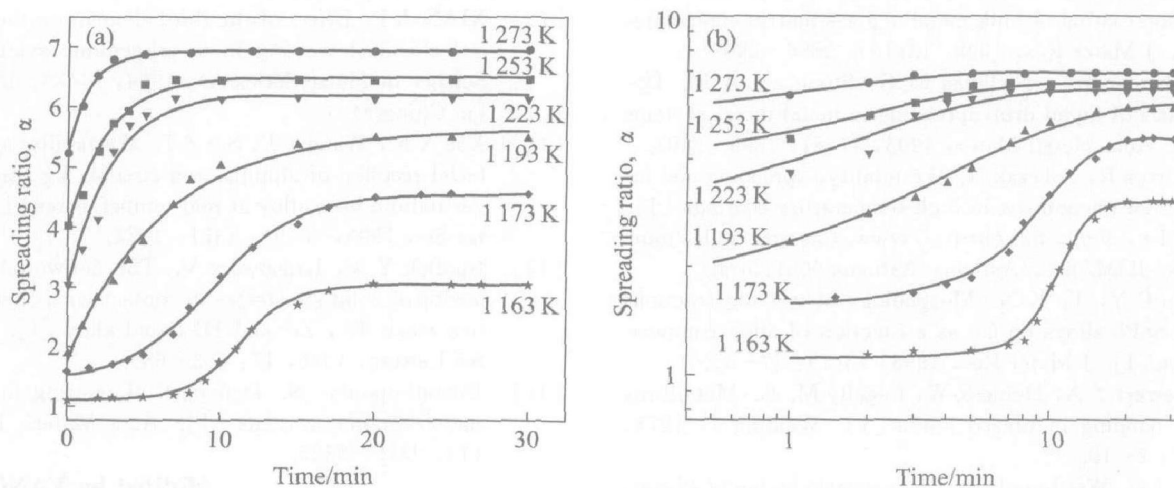
### 3.2 Spreading kinetics

Fig. 7 shows the spreading ratio curves for Zr<sub>55</sub>Cu<sub>30</sub>Al<sub>10</sub>Ni<sub>5</sub> melt on Al<sub>2</sub>O<sub>3</sub> at various temperatures, as plotted on a normal spreading ratio—normal time curve (Fig. 7(a)) and a logarithmic spreading ratio—logarithmic time curve (Fig. 7(b)). Similar to the contact angle curve shown in Fig. 1, the spreading ratio  $\alpha$  (Fig. 7(a)) can be seen to progress through three stages: incubation, quasi-steady increase and trend constant. Above 1 193 K incubation stage vanishes and the relationship between spreading ratio  $\alpha$  and spreading time is closed to the exponential function. At the quasi-steady increase stage, plot of  $\ln(\alpha)$  against  $\ln(t)$  at various temperatures gives approximately straight lines as shown in Fig. 7(b). The linear ranges are the so-called “quasi-steady spread range”<sup>[13]</sup>. The spreading ratio of molten Zr<sub>55</sub>Cu<sub>30</sub>Al<sub>10</sub>Ni<sub>5</sub> on Al<sub>2</sub>O<sub>3</sub> with the spreading time in this range can be given by



**Fig. 6** Spreading mechanism of molten Zr<sub>55</sub>Cu<sub>30</sub>Al<sub>10</sub>Ni<sub>5</sub> on Al<sub>2</sub>O<sub>3</sub>





**Fig. 7** Spreading ratio dependence of spreading time  $t$  for  $Zr_{55}Cu_{30}Al_{10}Ni_5$  molten on  $Al_2O_3$  at various temperatures

(a) —Linear time scale and linear spreading ratio scale; (b) —Logarithmic time scale and logarithmic spread ratio scale

$$(\alpha - a)^{1/n} = k(t - \tau) \quad (3)$$

where  $a$  and  $\tau$  are constants,  $k$  the spreading ratio constant ( $s^{-1}$ ) and  $n$  the spreading index, relating to the viscosity of the melt and the interaction between molten and interface.

Following the example of the treatment method of chemical reaction kinetics, plots of  $\ln k$  against  $1/T$  are shown in Fig. 8. The plot of  $\ln k$  against  $1/T$  is a straight line and follows Arrhenius behavior. Thus the apparent activation energy  $Q$  for spreading could be calculated from Fig. 8 and is about 156 kJ/mol. The molten metal spreading on the ceramic is chiefly affected by the viscosity of the melt, diffusion, interfacial reaction and the resulting triple line configuration. As mentioned above,  $Al_2O_3$  does not react with the molten  $Zr_{55}Cu_{30}Al_{10}Ni_5$  at the interface, but the formation of precursor film changes the triple line configuration. Thus the spread activation energy consists of three parts: the activation energy for the formation

of precursor film, the activation energy for the melt diffusion at the interface and that for the melt movement on precursor film.

#### 4 SUMMARY

Wetting behavior of molten  $Zr_{55}Cu_{30}Al_{10}Ni_5$  on alumina was studied. Due to the formation of precursor film when wetting temperature is higher than 1163 K,  $Zr_{55}Cu_{30}Al_{10}Ni_5$  molten spreads on  $Al_2O_3$  well. This is related to the change of triple line configuration. No reaction product has been detected at the interface. Thus,  $Al_2O_3$  is an excellent reinforcement for  $Zr_{55}Cu_{30}Al_{10}Ni_5$  bulk metallic glass matrix composite material in terms of wettability and reactivity.

#### REFERENCES

- [1] Asthana R. Reinforced cast metals: Part II evolution of the interface [J]. *J Mater Sci*, 1998, 33(8): 1959–1983.
- [2] Mortensen A. Interfacial phenomena in the solidification processing of metal matrix composites [J]. *Materials Science and Engineering A*, 1991, 135(3): 1–11.
- [3] Jadoon A K, Ralph B, Hornsby P R. Metal to ceramic joining via a metallic interlayer bonding technique [J]. *Journal of Materials Processing Technology*, 2004, 152: 257–265.
- [4] Naiditch J V. The wettability of solids by liquid metals [J]. *Prog Surf Membrane Sci*, 1981, 14: 353–421.
- [5] Choi Y H, Busch R, Köster U, et al. Synthesis and characterization of particulate reinforced  $Zr_{57}Nb_5Al_{10}Cu_{15.4}Ni_{12.6}$  bulk metallic glass composites [J]. *Acta Mater*, 1999, 47(9): 2455–2463.
- [6] Conner R D, Dandliker R B, Johnson W L. Mechanical properties of tungsten and steel fiber reinforced  $Zr_{41.25}Ti_{13.75}Cu_{12.5}Ni_{10}Be_{22.5}$  metallic glass matrix composites [J]. *Acta Mater*, 1998, 46(16): 6089–6090.

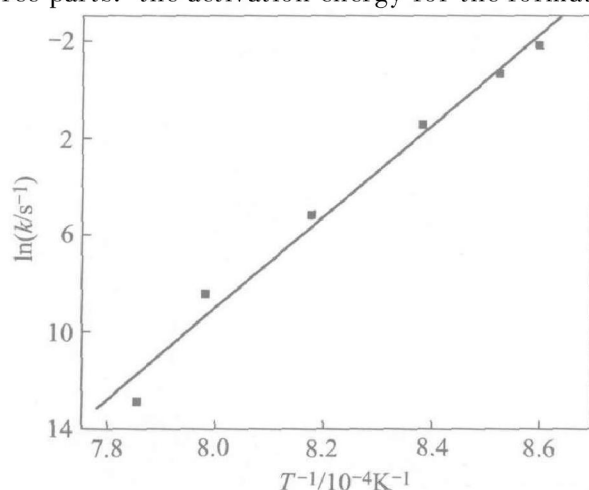


**Fig. 8** Variation of  $\ln k$  with  $1/T$  for spreading of molten  $Zr_{55}Cu_{30}Al_{10}Ni_5$  on  $Al_2O_3$

- [7] Dandliker R B, Conner R D, Johnson W L. Melt infiltration casting of bulk metallic glass matrix composites [J]. *J Mater Res*, 1998, 13(10): 2896 - 2903.
- [8] Amberose J C, Nicholas M G, Stoneham A M. Dynamics of liquid drop spreading in metal-metal systems [J]. *Acta Metall Mater*, 1993, 41(8): 2395 - 2401.
- [9] Asthana R, Sobczak N. Wettability, spreading and interfacial phenomena in high temperature coatings [J]. *JOM-e*, 2000, 52. (<http://www.tms.org/pubs/journals/JOM/0001/Asthana/Asthana0001.html>).
- [10] Liu C Y, Tu K N. Morphology of wetting reactions of SnPb alloys on Cu as a function of alloy composition [J]. *J Mater Res*, 1998, 13(1): 37 - 45.
- [11] Siewert T A, Heine R W, Lagally M. G. Metallurgy of bonding in brazed joints [J]. *Welding J*, 1978, 57: 2 - 10.
- [12] Li J G. Wetting of ceramic materials by liquid silicon, aluminium and metallic melts containing titanium and other reactive elements: a review [J]. *Ceramics International*, 1994, 20(6): 391 - 412.
- [13] XIAN A P. Effect of the third element on the interfacial chemical wetting in metal-ceramic system [J]. *Science in China (Series A)*, 1994, 24(3): 323 - 329. (in Chinese)
- [14] Xue X M, Wang J T, Sui Z T. Wettability and interfacial reaction of alumina and zirconia by reactive silver-indium base alloy at mid-temperatures [J]. *J Mater Sci*, 1993, 28(9): 1371 - 1374.
- [15] Naidich Y V, Krasovsky V. The nonwettability behavior of solid substrates in contact with chemical active reach Ti, Zr and Hf liquid alloy [J]. *J Mater Sci Letters*, 1998, 17: 683 - 685.
- [16] Eustathopoulos N. Dynamics of wetting in reactive metal/ceramic systems [J]. *Acta Mater*, 1998, 46(7): 2319 - 2325.

(Edited by YANG Bing)